99

Third International Symposium on

CABLE DYNAMICS

PROCEEDINGS

Trondheim (Norway), 16-18 August 1999

NON LINEAR FINITE ELEMENT MODELLING OF THE AEROELASTIC BEHAVIOUR OF A CABLE-STAYED STRUCTURE

Ir. N. Raimarckers, Pr. J-L. Lilien
Université de Liège, Institut d'Electricité Montefiore
B-4000 Sart Tilman (B28)
Tel:+32 4 366 26 33 – Fax:+32 4 366 2998 – E-mail: lilien@montefiore.ulg.ac.be, raimarck@montefiore.ulg.ac.be

INTRODUCTION

In this work, we want to propose a new approach of bridge finite element modelling. Based on mechanical characteristics and a limited number of aerodynamic coefficients, it intends to highlight the importance of cable dynamics in the whole structure behaviour.

The application chosen for this study is the Val-Benoît cable-stayed bridge (Belgium). We first compare the existing modal study results to the one of a conventional beam element model. Then we research the critical velocity for the flutter problem and finally estimate the most significant cable and deck movements under a 600 seconds turbulent wind load simulation.

Same model can be used to simulate rain-wind induced vibration, Von Karman vortex shedding effects and wake induced vibrations.

MODELLING

Turbulent wind with vertical profile

In addition to mean wind velocity spatially modulated by the vertical profile, presented in annexe, gusts impose a temporal variance to the speed.

Wind is never perfectly constant; turbulence affects the forces applied to the bridge deck not only through the module of instantaneous wind speed but also in function of their frequential content and of structure dynamics.

$$\mathbf{V}(\mathbf{p}, t)=\mathbf{V}(z)+\mathbf{u}^{fluct}(\mathbf{p}, t) \quad (2.1)$$

where u(p,t) is the along wind, v(p,t) crosswind and w(p,t) the vertical fluctuations. Figure 1 describes the typical energetic content

The gap in this spectrum allows us to treat short term variations as stationary. On the other hand, we notice that the first frequencies of civil structures are higher than the ones of the gusts peak; we can thus use a quasi-static approach for the buffeting problem.

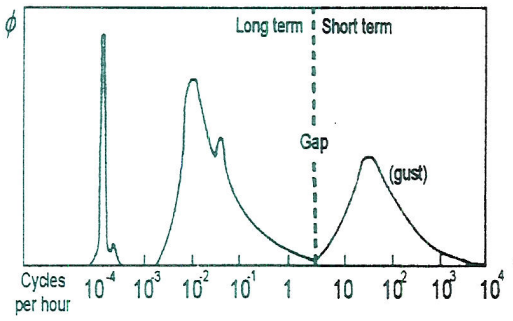

Fig. 1 : Power spectral density of wind velocity

The reference direction of the wind velocity is transversal, furthermore our model is line-like, the most important direction of fluctuation to correctly represent is u(p,t). Then

1) The most often met Power Spectral Densities able to model the wind in the high frequency domain are the ones of Davenport, Harris and Von Karman. Conjugated with the spatial correlation function $\eta(\Delta\mathbf{p}, \omega)$, these PSD define completely the wind two-dimensional random process.

$$\eta(\Delta p, \omega) = \exp\left(\frac{-\|\omega\|}{2\pi\|U\|} c_k \|\Delta p\|\right) \quad (2.2)$$

2) In vertical planes that contain the reference direction, the turbulence is assumed to be constant

The method used for the simulation of the samples is based on a modified wave superposition that was first proposed by M. Bocciolone et al. [9]. It's rather heavy from the computation time point of view but guarantees stability. We generates a discrete temporal sequence obtained by IFFT (Inverse Fast Fourier Transform) of discrete values of the spectrum.

$$u(p=0, t_k) = \sum_{n=0}^{N-1} \|C_n\| . \exp\left(i(\vartheta_n + \omega_n t_k)\right) \quad (2.3)$$

with

$$\|C_n\|^2 = \frac{2\pi}{N\Delta} S(\omega_n)$$

The spatial correlation function enables us to relate the phase of the different vertical planes

$$u(p=0,t_k)=\sum_{n=0}^{N-1}\|C_n\|.\exp\left(i(\varphi_n+\omega_n t_k)\right) \qquad (2.4)$$

with

$$\varphi_n = a\tan\left(\frac{\eta(\Delta p,\omega)\sin(\theta_n)+\sqrt{1-\eta^2(\Delta p,\omega}.\sin(\psi_n)}{\eta(\Delta p,\omega)\cos(\theta_n)+\sqrt{1-\eta^2(\Delta p,\omega}\cos(\psi_n)}\right)$$

where θ_n and ψ_n are sets of independent random angles uniformly distributed in $[0,2\pi]$.

Modelling of the bridge (deck and stays)

The Val-Benoît Bridge

The Val-Benoît Bridge is a concrete cable-stayed bridge which approach span is 30.5 meters and main span is 162 meters born by 22 cables meanwhile the retaining cables are anchored in the tunnel prolonging the bridge.

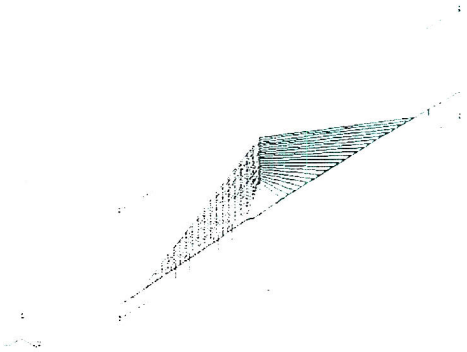

Figure 2: finite element model of the Val Benoît bridge

The characteristics of this bridge are:

1) a centred bundle of cables that permits nevertheless, thanks to the relative shortness of the building, to keep a good ratio (± 2) between the flexion and torsion first frequencies. The importance of this ratio in the prevention of flutter has been often evidenced.

2) a longitudinal freedom of movement of the pylon to enable dilatations since the tunnel is fixed.

Among the numerous frequencies of lateral cable vibration, we distinguish modes with a greater generalised mass corresponding to movements of the deck or of the pylon. We count as many as 50 modes below 1.59 Hz, so that the cables and structure modes are intimately mixed.

Furthermore, in this frequency band where we know wind excitation exists, some modes imply a composition of cables and deck (pylon) motions. So, our model that takes their interaction into account enables energy exchanges like parametric excitation.

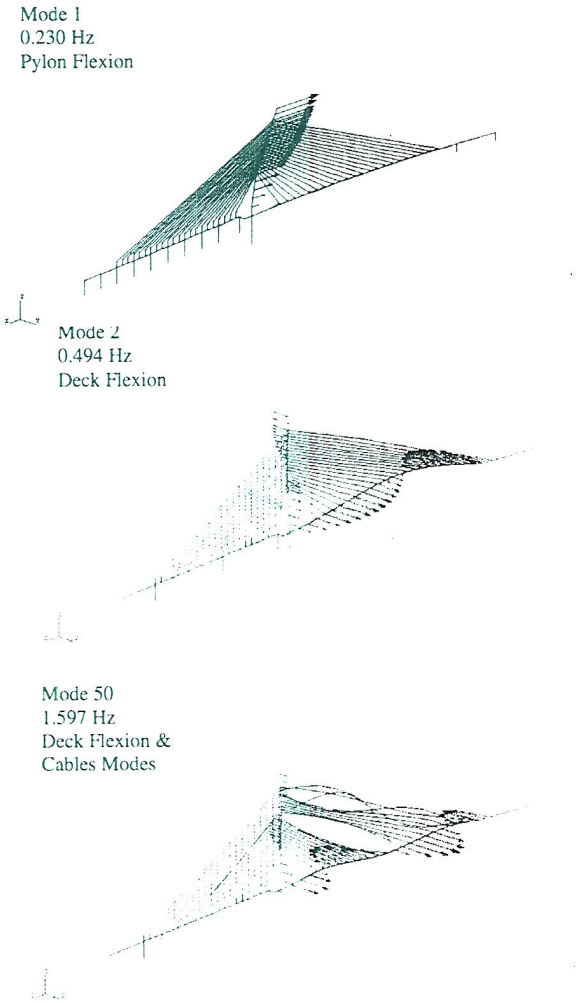

figure 3 : Mode shapes of the Val-Benoît bridge

In addition to the deformation the arrows length and direction in the above graphic represent the nodal rotation amplitudes. First two modes coincide with the conventional EF model ones even if their frequencies are slightly lower. The mode 50 is an example of strong coupling between the cables (not only on the first shape of the stays) and the other components.

Finite elements model

The computation technique is based on a finite elements model. The highly non linear behaviour of cables and of aerodynamic forces in terms of the degrees of freedom (dof) of the structures requires a temporal solution using of tangential stiffness. We use the direct method of temporal integration of Hilbert Hugues Taylor that brings damping to higher frequencies without degradation of the frequency domain of interest (under 5Hz).

An improvement could be brought to this formulation since an inclined cable even under horizontal oblique wind possess an apparent elliptical section with a non-zero angle of incidence.

The short axe in the Z_1 direction remains equal to D but the long axe in the Y_1 direction is

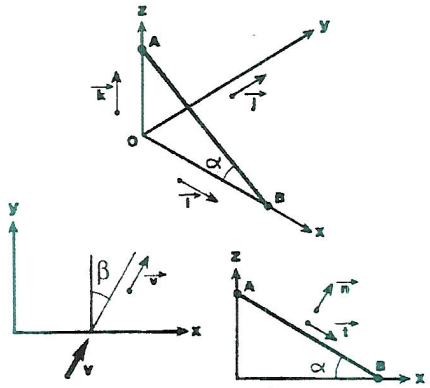

Figure 6 : Horizontal oblique wind on inclined cable

multiplied by $\sqrt{1+\frac{\sin^2\beta}{\cos^2\beta}\cos^2\alpha}$ (3.2)

as showed by M.Virlcgeux [4] and the γ angle of attack is given by $\sin\gamma = \sin\alpha \,.\, \sin\beta$
where α is the inclination of the cable and β the angle between V_{MOYR} and axis y.

The previous improvement requires aerodynamic curves for different elliptic axis ratios obtained by experimental measures or numerical simulations.

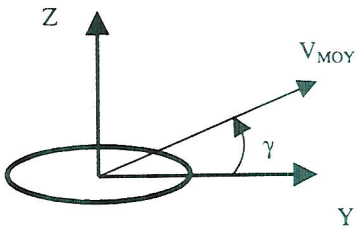

figure 7 : Apparent elliptical section and incidence angle

Buffeting Forces

Effects of turbulent component of the wind velocity are not only characterised by its magnitude and direction but also by its frequency spectrum and wave length. That's why we separate this effect from the mean force one and we use aerodynamic admittance coefficients to take into account the non line-like shape of bridge.

The difference between absolute instantaneous and mean wind velocities in the cross section plane expressed in local axes gives the turbulent resultant. We get the usual speeds: u in the direction of absolute mean wind and w perpendicular to it.

The expression of the linearised buffeting forces in the mean wind reference is:

$$L_b = \frac{1}{2}\rho V_{MOY}^2 D\left[2C_L\frac{u}{V_{MOYA}} + \left(\frac{dC_L}{d\gamma} + C_D\right)\frac{w}{u}\right]$$

$$M_b = \frac{1}{2}\rho V_{MOY}^2 D^2\left[2C_M\frac{u}{V_{MOYA}} + \left(\frac{dC_M}{d\gamma}\right)\frac{w}{u}\right] \quad (3.3)$$

$$D_b = \frac{1}{2}\rho V_{MOY}^2 D\left[2C_D\frac{u}{V_{MOYA}} + \left(\frac{dC_D}{d\gamma} + C_L\right)\frac{w}{u}\right]$$

We have seen that gust spectrum guarantees for civil building a good accuracy to the quasi-static hypothesis. However, the aerodynamic admittance coefficients allow a dynamic correction to consider the correlation of forces on the pylon and on the deck.

The aerodynamic admittance response (Sears function) for a thin symmetrical airfoil is analytically expressed in Bessel functions and can be approximated by

$$\chi^2_{Sears}(n) = \frac{1}{1+2\pi^2(nD/V_{MOYA})} \quad (3.4)$$

where n is the frequency of the turbulence and D is the width of the deck. The admittance function only depends on the ratio $\frac{nD}{V_{MOYA}}$ (Strouhal number) since it takes into account an unsteady flow problem.

Semi-empirical formulae have been developed by Davenport for bridges sections like

$$\left\|\chi_i(\omega)\right\|^2 = \frac{2\left[\lambda B_i - 1 + \exp(-\lambda B_i)\right]}{(\lambda B_i)^2} \quad (3.5)$$

with $\lambda = \frac{7\omega}{2\pi V_{MOYA}}$ and B_i : characteristic lengths.

For the cables, the time required for the fluid particle to pass along the cross section is so short in comparison to the vibrating period that the flow pressure is not influenced by this movement. The quasi static assumption is thus accurate and we can simply replace V_{MOY} by V_{INST} and the mean angle of attack γ by its instantaneous value in (3.1) and in the definition of φ.

Motion induced Forces

The adimensional number ruling the behaviour of a flow where a moving body is plunged is the Strouhal. We see that its very little value (0.02) for cables justifies a quasi-static approach (relative speed) while it's approximately equal to one for the deck and requires a complete dynamic aeroelastic solution.

$$Str = \frac{T_{sec\ tion}}{T_{galop}} = \frac{\left(\frac{D_{cable}}{V_{MOY}}\right)}{\left(\frac{1}{f_{galop}}\right)} \approx \frac{1Hz * 0.1m}{5m/s} \approx 0.02$$

$$Str = \frac{T_{tablier}}{T_{galop}} = \frac{\left(\frac{D_{tablier}}{V_{MOY}}\right)}{\left(\frac{1}{f_{galop}}\right)} \approx \frac{0.5Hz * 30m}{15m/s} \approx 1$$

The most common expression of aeroelastic force terms is the following one developed by Scanlan and Tomko:

$$L_{ae} = \frac{1}{2}\rho V_{MOYA}^2 D\left[KH_1^* \frac{h}{V_{MOYA}} + KH_2^* \frac{D\dot{\vartheta}}{V_{MOYA}} + K^2 H_3^* \vartheta + K^2 H_4^* \frac{h}{D}\right]$$

$$M_{ae} = \frac{1}{2}\rho V_{MOYA}^2 D^2\left[KA_1^* \frac{h}{V_{MOYA}} + KA_2^* \frac{D\dot{\vartheta}}{V_{MOYA}} + K^2 A_3^* \vartheta + K^2 A_4^* \frac{h}{D}\right]$$

$$D_{ae} = \frac{1}{2}\rho V_{MOYA}^2 D\left[KP_1^* \frac{h}{V_{MOYA}} + KP_2^* \frac{D\dot{\theta}}{V_{MOYA}} + K^2 P_3^* \vartheta + K^2 P_4^* \frac{h}{D}\right] \quad (3.6)$$

with K=Dω/U=Str and $H^*_i(K)$, $A^*_i(K)$, $P^*_i(K)$ "flutter derivatives" experimentally determined. h and θ are respectively the vertical movement and the angle of torsion of the deck relative to the static equilibrium position.

We work in the time domain so we take the Inverse Fourier transform of the formulation based on transfer functions proposed by Bucher and Lin:

$$F_{M\vartheta}(\omega) = \rho D^2 V_{INSTA}^2 \left[C_{1M\vartheta} + \frac{D}{V_{INSTA}} i\omega C_{2M\vartheta} + \sum_{k=3}^{n} C_{kL\vartheta} \frac{i\omega}{d_{kM\vartheta}\frac{V_{MOYA}}{D} + i\omega}\right] \quad (3.7)$$

$$M_{\vartheta}(t) = \rho D^2 V_{INSTA}^2 \left\{\left[C_{1M\vartheta}\vartheta + \frac{C_{2M\vartheta}B}{V_{MOYA}}\dot{\vartheta}\right] + \sum_{k=3}^{n} C_{kM\vartheta} \int_{-\infty}^{t} \exp\left(-\frac{d_{kM\vartheta}V_{MOYA}}{D}(t-\tau)\right)\dot{\vartheta}(\tau)d\tau\right\} \quad (3.8)$$

Similar expressions define moment, drag and lift aerodynamic coefficients in function of θ and h and

$$\begin{cases} M_{ae} = M_{\vartheta}(t) + M_h(t) \\ L_{ae} = L_{\vartheta}(t) + L_h(t) \\ D_{ae} = D_{\vartheta}(t) + D_h(t) \end{cases} \quad (3.9)$$

We have first verified our implementation of flutter forces by comparing our results with the ones of an analytical root-locus method. We have considered the simple case of a rigid section mounted on vertical and torsion springs and dampers. The aeroelastic and dynamic coefficients presented in annexe used are the characteristics of the reduced model of the Bridge of the Tage.

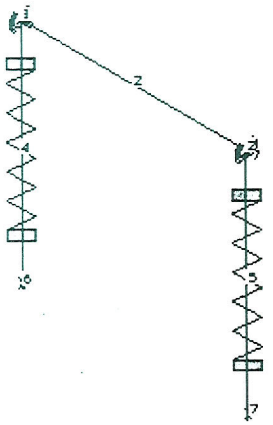

Figure 8 : Aeroelastic profile
mounted on flexion and torsion springs and dampers

The root locus calculation determines a critical velocity of 15m/s. Above this wind speed, the torsion mode is unstable what means that vibrations are self sustained and amplified.

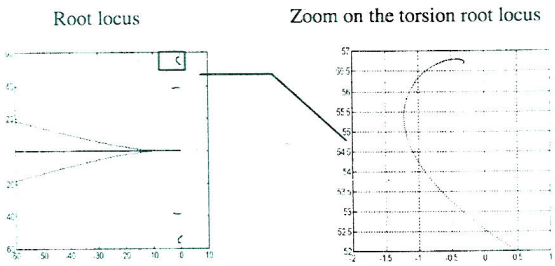

Figure 9 : Root-Locus

This verification is successful, since for different increasing speeds, we note the following comportment:

1) a slower and slower decay of torsion vibrations until 10m/s. Above 10 m/s, the amplitude is approximately constant and after 20 m/s, we note a fast increasing. It corroborates the root-locus procedure results since torsion roots rapidly moves in direction of the right unstable plane.

2) the flexion vibrations decay faster and faster. This confirm the movement of flexion pole towards left in the speed domain of interest.

The graphics of the flexion and torsion vibration amplitudes for an increasing speed [0-20m/s] achieve the validation. After a rapid decay of the initial perturbation for speeds under 8m/s, amplitude of torsion remains constant until about 17 m/s and quickly increases after. The decay of flexion vibrations increases with wind speed.

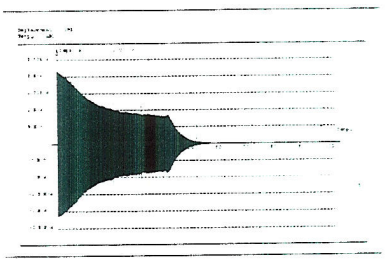

Figure 9 : Flexion vibration amplitudes

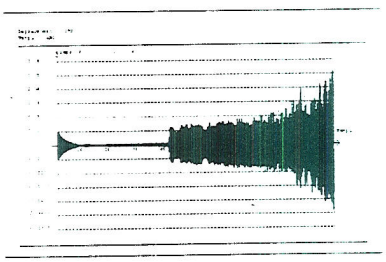

Figure 10 : Torsion vibration amplitudes

Aeolian vibrations

Aeolian vibration designates the lateral motions perpendicular to the wind velocity induced by alternated Von Karman wakes. The coincidence of the aeolian $f_{aeolian} = \frac{Str.V_{MOYR}}{D}$ $(Str \in [0.185,0.2])$ and cable natural frequencies results in larger motions and the lock-in effect.

Most frequent energy balance models cannot be used in our finite element formulation. In the future, we intend to apply a *lift-oscillatory* model whose essential properties have been deduced from experimental results:

.limited periodic lift forces appear on a steady cylinder so that oscillator has to be self-excited and self-limited

.natural frequency must be proportional to wind velocity.

.cable movement must interact with oscillator through an excitation term.

We will add to the other wind excitations a lift force responding to the equation :

$$\ddot{C}_L - \alpha_1 \dot{C}_L + \gamma_1 \left(\dot{C}_L\right)^3 + \omega_0^2 C_L = f\left(\dot{h}\right) \quad (3.10)$$

Applications

There are two main simulation type for which we have measured displacements and other nodal and element characteristics.
In the first one, the structure is plunged into a non turbulent but increasing speed from 0 to 25 m/s. The cables stays aerodynamic coefficients are set to zero, so that, after initial excitation, aerodynamic forces acting on the deck and the pylon are the only extern ones. This situation is very interesting to study flutter behaviour and cable excitation by deck motions.
We consider, for the second one, a turbulent wind velocity with a vertical profile acting on the structure during 600s. Its main characteristics are v_G 15m/s, site ground roughness type 3, turbulence 5%.

However, we still miss coherent aerodynamic and aeroelastic data for this bridge. Further results will be presented at the conference.

ANNEXE

Modelling of the wind

The problem generality requires us to consider a time dependant tridimensional wind velocity field **V**(x,t).

$$\mathbf{V}(x,t) = \begin{bmatrix} u(x,t) \\ v(x,t) \\ w(x,t) \end{bmatrix} \quad (4.1)$$

In the next sections we will explain different models used to render time and spatial variations of this field.

Mean wind velocity

The principal characteristic of wind is its mean value since it regulates most of aerodynamic excitations.

$$\mathbf{V}_{moy}=E[\mathbf{V}(x,t)] \qquad (4.2)$$

The direction transversal to the structure creates the strongest excitations, it will be chosen as the reference direction.

Vertical Profile

The presence of the ground creates a boundary layer in the atmosphere movements and thus a strong dependence of the wind field with the altitude z. We can consider that the mean wind speed direction doesn't change with the altitude, the mean speed profile varies essentially with the ground roughness.

The principal models are based on empirical laws but are however fairly accurate.

Power Law

$$V(z)=V_G\left(\frac{z}{z_G}\right)^{\beta} \qquad (4.3)$$

Logarithmic Law

$$V(z)=c.\ln\left(\frac{z}{z_0}\right)V_G \qquad (4.4)$$

where the constants β, z_G, c et z_0 depend of the roughness of the type of site.

Site Description	Site Type	β	z_g	c_k	z_0
Sea	I	0.11	250	0.166	0.005
Countryside	II	0.19	317	0.202	0.07
Rural area	III	0.27	390	0.234	0.3
Industrial area	IV	0.34	450	0.266	1
Centre of large towns	V	0.38	494	0.292	2.5

z_G is the gradient altitude i.e. above which the effect of the boundary layer is negligible. V_G is the corresponding velocity and thus represent the wind speed calculated by an ideal fluid model and is independent of the type of the site.

In the case we study, the site type is classed 3, and β=0.27, z_G=390 meters and the top of the bridge is 87 meters high so that V varies from 0 at the ground level at the bottom of the pylon and .4*v_G at the deck height to 0.820*v_G. This influence is then not negligible on the whole of cable span.

Dynamic and Aeroelastic coefficients

M=4.6kg, I=.062kg.m² , f_h=6.19Hz, ξ_h=0.00054, f_α=9.02Hz, ξ_α=.0057

	C_1	C_2	C_3	C_4	d_3	d_4
M_α	0.279	0.131	19.78	-21.37	1.715	1.991
M_h	0	0	0	0	0	0
L_α	0	0	0	0	0	0
L_h	1.128	-2.292	-0.985	-1.102	1.593	0.821

NOTATIONS

N: number of points in the temporal sequence
Δ : sampling period
$\omega_n=2\pi n/(N\Delta)$: interval in the frequency sequence
$T_a=N.\Delta$: Period of observation (600 s.)

C: gravity centre position of the cable cross section
i : gravity centre position of the rain rivulet
G: gravity centre position of the total cross section
$\mathbf{n}(s_0,t)$: normal unit vector to the cross section
$\theta(s_0,t)$: rotation vector in tangential direction
$\theta_i(s_0)$: angle between $\mathbf{t}_2$ and the line passing trough C and i.

V_{MOYR} : relative mean speed vector
V_{MOYA} : absolute mean speed vector
V_{INSTR} : relative instantaneous speed vector
V_{INSTA} : absolute instantaneous speed vector
U,V,W : projected velocity on element axis X,Y,Z respectively

L, D, M : Lift, Drag and Moment aerodynamic coefficients
$_{ae}$: aeroelastic
$_b$: buffeting

BIBLIOGRAPHY

1. Keutgen Renaud, *Galloping phenomena, a finite element approach.* Ph. D. thesis, Collection des publications de la faculté des sciences appliquées, n°191, Université de Liège, 05/1999 .
2. R.H. Scanlan, *Wind dynamics of long-span bridges, Aerodynamic of large bridges*, Proceedings of the first International Symposium on Aerodynamic of Large Bridges, pp 47-57, Danish maritime institute, ed. A Larsen, 02/1992
3. C.Dyrbye & S.O.Hansen, *Wind load on structures*, ed. John Wiley & Sons pp 143-172, 1997
4. M. Virlogeux, *Cable vibration in cable stayed bridges, Bridge Aerodynamics*, Proceedings of the international symposium on advances in bridge aerodynamics, pp 213-234, ed. A. Larsen & S. Esdahl, 05/1998